Calorimetric Investigation of the Domain Structure of Human Complement C1s: Reversible Unfolding of the Short Consensus Repeat Units†

Leonid V. Medved,‡ Thomas F. Busby, and Kenneth C. Ingham*
Biochemistry Laboratory, American Red Cross Biomedical Research and Development, Rockville, Maryland 20855
Received December 9, 1988; Revised Manuscript Received March 8, 1989

ABSTRACT: C1s is a multidomain serine protease that participates in Ca^{2+}-dependent protein–protein interactions with other subcomponents of C1, the first component of human complement. Proteolytically derived fragments that retain some of the functional properties of the parent protein have been isolated, and their thermal stability has been investigated by differential scanning calorimetry. Three endothermic transitions are observed in whole C1s near 37, 49, and 60 °C in 0.05 M Tris-HCl, pH 7.2, containing 0.22 M NaCl and 0.1 mM EDTA. The first (37 °C) and third (60 °C) transitions are also seen in C1s-A, a derivative comprised mainly of the intact nonenzymatic A chain. The second (49 °C) and third transitions are seen in C1s-γB, a fragment comprised of the intact B chain, disulfide linked to the C-terminal γ region of the A chain. Thus, the first transition, which is alone stabilized by Ca^{2+}, corresponds to the melting of the N-terminal αβ region of the A chain, the second to the melting of the catalytic B chain domain, and the third to the γ region. The γ region is comprised of two homologous short consensus repeat (SCR) motifs that are also found in several other complement and coagulation proteins. A new 24-kDa fragment, C1s-γ, which contains these two SCRs, was isolated from plasmic and chymotryptic digests of C1s-A. C1s-γ exhibits a reversible transition near 60 °C corresponding to the highest temperature peak in whole C1s and C1s-A. The denaturation process of C1s-γ, which is characterized by a calorimetric to van't Hoff enthalpy ratio of 2.1, involves two independent two-state transitions, indicating that the two SCRs melt independently and are therefore independently folded. The C1s molecule is therefore comprised of at least four independently folded domains: one or more in the αβ region, two in the γ region, and one in the catalytic B chain.

C1s is one of three constituents of the first component of complement [reviewed by Cooper (1985), Schumaker et al. (1987), and Arlaud et al. (1987)]. Upon activation, it is converted from a single-chain zymogen to a two-chain serine protease, designated C1s, that is the catalytic unit of C1-esterase. At least two domains have been observed in the electron microscope: a catalytic domain comprised of the light B chain together with a C-terminal γ region of the heavy A chain and a regulatory or interaction domain located in the N-terminal region of the A chain (Villiers et al., 1985). In previous studies of the stability of C1s and its homologous partner, C1r, fluorescence probes and other methods were used to characterize two thermal transitions in each protein, a low-temperature Ca^{2+}-sensitive transition arising from the interaction domain and a high-temperature Ca^{2+}-insensitive transition arising from the catalytic domain. These assignments were confirmed by the demonstration of analogous transitions in functional fragments isolated from proteolytic digests of the parent proteins (Busby & Ingham, 1987, 1988).

Differential scanning calorimetry measurements by Lennick et al. (1985) provided evidence for a third transition in C1s at a higher temperature than the two transitions detected by the fluorescence probes. The primary structures of C1r and C1s contain a number of sequence "motifs" that also suggests the existence of additional domains beyond those responsible for the two transitions already characterized (Figure 1). The A chain of each protein contains an epidermal growth factor like structure (motif II) similar to those found in some coagulation proteins (Stenflow et al., 1987) as well as two pairs of internally homologous repeat structures. One of these repeats (motifs I and III) is unique to C1r and C1s, while the other (motifs IV and V) is similar to the so-called short consensus repeat (SCR) motifs found in several complement and other proteins (Reid et al., 1986; Klickstein et al., 1987). For example, each of the seven chains of C4b binding protein contains 8 contiguous SCRs, the b subunit of clotting factor XIII contains 10, and the C3b/C4b receptor contains 30. The occurrence of such structures in multiple copies in such a wide variety of proteins raises interesting questions regarding the evolution of protein structure and the relationship between these sequence motifs, often referred to in the literature as domains, and true structural domains that are independently folded and whose unfolding can be observed under appropriate conditions. Should each of these motifs be assumed to be independently folded, or are their three-dimensional structures determined by mutual interactions between motifs?

The ultimate proof of the existence of independently folded domains within a protein is their successful isolation from a proteolytic digest combined with a demonstration of their structural integrity through studies of their unfolding. Differential scanning calorimetry is one of the best approaches to examining domain structure, as reviewed by Privalov (1979, 1982). In the present study we have further characterized the melting behavior of C1s by this method. In addition to confirming some of the earlier results obtained by fluorescence methods, we have shown that the third transition detected by Lennick et al. (1985) has its origin in the C-terminal region of the A chain. A fragment containing motifs IV and V was isolated from a plasmin digest of C1s and shown to be responsible for this transition. Careful analysis of the melting behavior of this and other fragments in comparison to that of the intact protein allowed us to conclude that the C1s molecule is comprised of at least four independently folded domains.

† Supported in part by National Instituted of Health Grant HL21791.
* To whom correspondence should be addressed.
‡ Permanent address: Institute of Biochemistry, Academy of Sciences of the Ukrainian SSR, Kiev 252030, USSR.

0006-2960/89/0428-5408$01.50/0

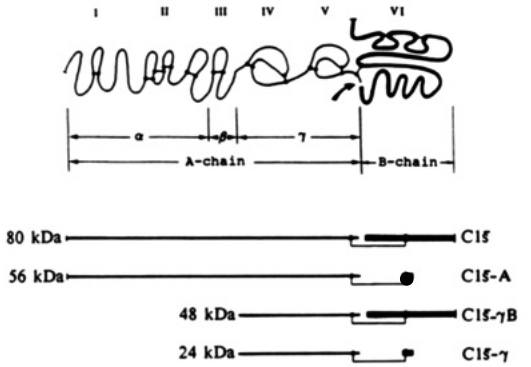

FIGURE 1: Schematic representation of C1s̄ and its fragments. The Roman numerals refer to different motifs identified in the primary structure (Tosi et al., 1987; Mackinnon et al., 1987). α, β, and γ refer to different proteolytic fragments (Villiers et al., 1985).

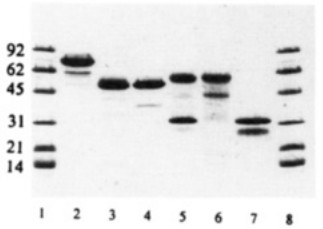

FIGURE 2: Analysis of C1s̄ and its fragments by SDS–PAGE. Lanes 2–4 were nonreduced samples, and lanes 5–7 were reduced prior to electrophoresis. (Lanes 1 and 8) Molecular weight standards; (lanes 2 and 5) C1s̄; (lanes 3 and 6) C1s̄-A fragment; (lanes 4 and 7) C1s̄-γB fragment. The lower band in lane 6 represents the presence of a specific cleavage in some of the C1s̄-A molecules, as previously described (Busby & Ingham, 1988).

The results obtained clearly show that each SCR unit (motif IV and V) in C1s̄ is folded independently.

Materials and Methods

C1s̄ was purified from Cohn fraction I of human plasma by affinity chromatography according to the method of Bing et al. (1980), except that the IgG–Sepharose was prepared according to the method of Kolb et al. (1979). C1s̄-A and C1s̄-γB fragments (Figure 1) were prepared as described earlier (Busby & Ingham, 1988). The purity of C1s̄ and its fragments was analyzed by size exclusion chromatography (Busby & Ingham, 1988) and SDS–polyacrylamide gel electrophoresis (SDS–PAGE) before and after reduction (Figure 2). SDS–PAGE was performed in 8–25% gradient polyacrylamide gels on a Pharmacia Phast System, and the proteins were visualized with Coomassie blue. The C1s̄ contained small amounts of a smaller species, possibly a degradation product, which is visible in heavily loaded gels (Figure 2, lane 2). The lower band in lane 6 of Figure 2 represents the presence of a specific cleavage in some of the C1s̄-A molecules, as previously described (Busby & Ingham, 1988).

The concentrations of protein solutions were determined spectrophotometrically by using the following values of $E_{280,1\%}$: 13.7 for C1s̄; 11.9 for C1s̄-A fragment; 17.7 for C1s̄-γB fragment (Busby & Ingham, 1988); and 17.4 for C1s̄-γ fragment. The $E_{280,1\%}$ value for the C1s̄-γ fragment (17.4) was calculated by the method of Edelhoch (1967) using a molecular mass of 23.4 kDa calculated from the sum of the amino acids of the γ region (Mackinnon et al., 1987; Tosi et al., 1987), the B chain remnant (Busby & Ingham, 1988), and 50% of the carbohydrate (Sim et al., 1977). The molecular masses of C1s̄ (80.3 kDa), C1s̄-A fragment (56 kDa), and C1s̄-γB fragment (48 kDa) have been calculated earlier (Busby & Ingham, 1988).

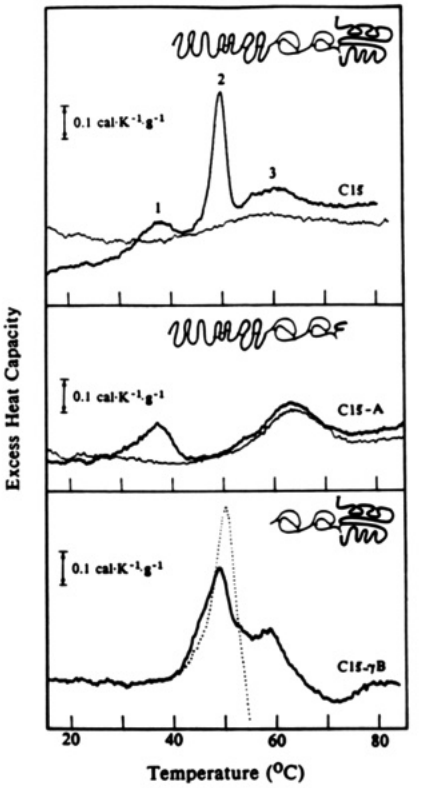

FIGURE 3: Differential scanning calorimeter recordings of the melting curves of C1s̄, C1s̄-A fragment, and C1s̄-γB fragment. C1s̄ and C1s̄-A were first heated (thick line) and then cooled and reheated (thin line) to check the reversibility of the melting transitions. The solvent was 0.05 M Tris-HCl, pH 7.2, 0.22 M NaCl, and 0.1 mM EDTA, except for the lower curves for C1s̄-γB which correspond to pH 7.2 (dotted line) and pH 8.0 (thick line).

N-Terminal protein analyses of the fragment were performed on a Beckman System 890M sequencer. Subsequent PTH amino acids were analyzed on a Waters HPLC system equipped with a Zorbax ODS C-18 reverse-phase column using a pH 5.0 sodium acetate/acetonitrile gradient.

Calorimetric measurements were made on a MicroCal MC-2 differential scanning calorimeter at a heating rate of 1 K/min and at a protein concentration of 1–3 mg/mL. The solvent conditions were carefully chosen to minimize aggregation of the denatured protein. Unless otherwise indicated, the melting curves presented were obtained in 0.05 M Tris-HCl, pH 7.2, 0.22 M NaCl, and 0.1 mM EDTA buffer, and aggregation was not observed upon heating a solution of C1s̄ or its fragments up to 90 °C; i.e., solutions remained clear after heating, and exothermic effects were minimal. However, the γB fragment showed a strong tendency to aggregate under these conditions and became turbid upon heating; therefore, no attempt was made to extract thermodynamic parameters from its melting curve. All curves have been corrected for the instrumental base line obtained by heating solvent in the absence of protein. Each melting curve was obtained at least twice with separate samples to ensure reproducibility of the results. The partial heat capacity of the proteins and the molar calorimetric (ΔH_m^{cal}) and van't Hoff enthalpy (ΔH_m^{vh}) were determined as described earlier (Privalov & Khechinashvili, 1974; Privalov & Medved, 1982). Deconvolution of excess heat capacity functions was performed by the recurrent procedure of Freire and Biltonen (1978) using software available from MicroCal.

Results

Melting of C1s̄ and Its Fragments. The thick traces in Figure 3 represent the temperature dependence of the partial

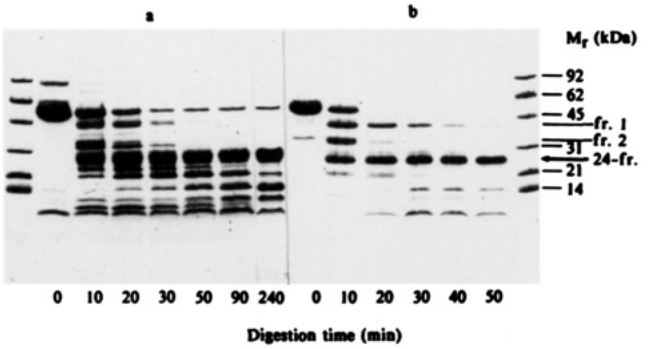

FIGURE 4: Digestion of C1s̄-A fragment with plasmin and chymotrypsin. Nonreduced samples were examined by SDS–PAGE in 8–25% gradient gels after digestion with plasmin (a) and chymotrypsin (b) for various times at 37 °C in 0.05 M Tris-HCl, pH 7.2, 0.22 M NaCl, and 0.1 mM EDTA. C1s̄-A concentration was 3 mg/mL, and the enzyme/C1s̄-A ratio was 1/100 (w/w). fr.1 and fr.2 designate two intermediate fragments, and 24-fr. refers to the final product, C1s̄-γ.

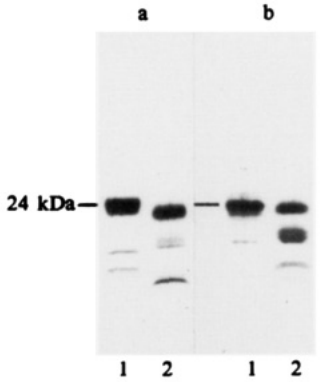

FIGURE 5: Analysis of the purified 24-kDa C1s̄-γ fragment by SDS–PAGE. C1s̄-γ was purified from a digest of C1s̄-A with plasmin (a) and chymotrypsin (b). Nonreduced (lanes 1) and reduced (lanes 2) samples were analyzed in 8–25% gradient gels.

heat capacities of C1s̄ and its fragments, C1s̄-A and C1s̄-γB. There are three intensive heat absorption peaks in the whole protein, two in C1s̄-A, and one or two in C1s̄-γB depending on the conditions. The latter fragment showed a strong tendency to aggregate during its first transition near 50 °C, obscuring the next transition. This effect was less severe at pH 8.0. From a comparison of the melting profiles obtained for the whole molecule with those of its fragments, it is evident that the observed transitions correspond to the separate melting of different parts of the molecule that differ in thermostability. It follows then that there are at least three different regions of compact structure in the C1s̄ molecule that melt independently with intensive heat absorption in different temperature ranges.

The first peak is observed in C1s̄ and C1s̄-A but not in C1s̄-γB. Since the γB fragment differs from C1s̄ by the absence of the N-terminal portion of the A chain, including the α and β regions (Figure 1), it can be concluded that the structures that melt in this temperature range are found within these regions. The second peak corresponds to the melting of some structure formed by the B chain, because it is prominent in C1s̄-γB but absent in C1s̄-A, which lacks most of the B chain (Figure 1). As for the third high-temperature peak, it must correspond to the melting of the γ region of C1s̄ because of its presence in the melting profiles of C1s̄-A and C1s̄-γB (pH 8.0), both of which contain this region.

The first and second peaks in C1s̄ and the first peak in C1s̄-A were not reproduced when these proteins were heated a second time (Figure 3, thin traces). The third peak in C1s̄ was partially reproduced, and the corresponding peak in C1s̄-A was almost completely reproduced in the second heating. The absence of the B chain and its corresponding transition in C1s̄-A enhances the prominence of transition 3 in this fragment as compared to the parent protein and shifts the apparent midpoint upward by 3.5 °C.

Preparation of the Thermostable Region of C1s̄. The above results suggest that the γ regrion of C1s̄ is the most thermostable part of the molecule under the conditions used and, one might assume, the most resistant to proteolysis. This suggests a parthway for the isolation of the thermostable γ region from the C1s̄-A fragment. As has been shown previously (Medved et al., 1982), the part of a protein with the lower thermostability can be easily removed if the protein is treated with a proteolytic enzyme under conditions in which this part is unfolded, while the thermostable part remains compact and resistant to proteolysis. For C1s̄-A, such conditions can be achieved by incubating the fragment at 37 °C, close to the midpoint of the first transition (Figure 3).

The time courses for digestion of the C1s̄-A fragment by plasmin and chymotrypsin are presented in Figure 4. Both enzymes rapidly generate a 24-kDa fragment that is highly resistant to further proteolysis. This fragment was purified from a 4-h plasmin and a 1-h chymotrypsin digest by size exclusion chromatography on a Superose 12 column (Pharmacia). The resulting products show a single major band by SDS–PAGE before reduction (Figure 5, lanes a1 and b1). After reduction, the fragment derived from the plasmin digest remained mostly intact (Figure 5, lane a2), whereas that from the chymotrypsin digest yielded larger amounts of low molecular weight bands (Figure 5, lane b2). These results suggest that there were several internal clips in a portion of the chymotryptic 24-kDa fragment preparation and that the resulting peptides were held together by disulfide bonds.

N-Terminal sequence analysis of the plasmic 24-kDa fragment produced two major sequences, Leu_{270}–Phe_{278} and Met_{526}–Leu_{535}, and a minor sequence, Gly_{196}–Arg_{205}. The latter sequence is found between the α and β regions and probably accounts for the low molecular weight contaminants that were detected by SDS–PAGE (Figure 5, lane a1). The second major sequence is also present in the parent C1s̄-A fragment and corresponds to the small remnant of the B chain with an M_r of less than 4000 that is attached to the A chain by a disulfide bond (Busby & Ingham, 1988). Its presence is consistent with the slight decrease in apparent size on SDS–PAGE following reduction (Figure 5, lanes a1 vs a2). The first sequence indicates that plasmin cleaves the Lys_{269}–Leu_{270} bond, between the β and γ regions, to produce a 24-kDa fragment composed of the γ region attached to the small B chain remnant (Figure 1). The molecular mass of this fragment calculated from the amino acid sequence (23.4 kDa) is in good agreement with that determined by SDS–PAGE. Since the 24-kDa fragment derives from the γ region of the C1s̄-A fragment, we refer to it as C1s̄-γ.

The melting curve for the plasmin-derived C1s̄-γ fragment is shown in Figure 6. It exhibits a single transition with a midpoint of 61 °C, close to that of transition 3 in whole C1s̄ and the corresponding transition in C1s̄-A, with a clearly determined change in heat capacity between the native and denatured states, $\Delta_m C_p$. The transition is highly reversible; a second heating produced an endotherm that was almost identical with the first. Similar results were obtained with the chymotrypsin-derived fragment (not shown). These observations prove unequivocally that the third peak in C1s̄ has its origin in the γ region.

Table I: Thermodynamic Characteristics of the Melting of C1s̄ and Its Fragments[a]

protein	peak 1				peak 2				peak 3			
	T_m	ΔH_m^{cal}	ΔH_m^{vh}	R	T_m	ΔH_m^{cal}	ΔH_m^{vh}	R	T_m	ΔH_m^{cal}	ΔH_m^{vh}	R
C1s̄	37.3	79	82	1.0	49.2	139	195	0.7	59.5	107	66	1.6
C1s̄-A	36.7	60	87	0.7					63.0	104	62	1.7
C1s̄-γ									61.0	135	65	2.1

	T_m	ΔH	T_m	ΔH	T_m	ΔH	T_m	ΔH
C1s̄	37.0	73	49.0	150	59.8	57	61.5	53
C1s̄-A	35.8	66			61.3	47	63.0	54
C1s̄-γ					58.1	65	62.8	66

[a] The upper portion of the table is based on the manual analysis in Figure 7, and the lower portion is based on the deconvolution analysis of Figure 8 (see text). T_m is the midpoint of the transition in degrees Celsius. ΔH_m^{cal} and ΔH_m^{vh} are the calorimetric and van't Hoff enthalpies. R is the ratio, $\Delta H_m^{cal}/\Delta H_m^{vh}$. In the lower part, only one value of ΔH is given since $\Delta H_m^{cal} = \Delta H_m^{vh}$ for the two-state transitions obtained by the deconvolution analysis. Experimental error is estimated to be ±1 °C in T_m and ±5% in ΔH values.

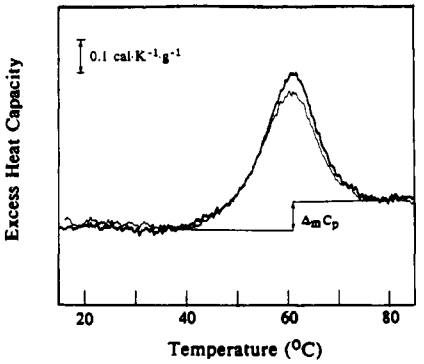

FIGURE 6: Differential scanning calorimetric recording of the melting curve of the plasmin-derived 24-kDa C1s̄-γ fragment. The sample was heated under conditions identical with those for C1s̄ and C1s-A in Figure 3 (thick line), cooled, and reheated under the same conditions (thin line). $\Delta_m C_p$ designates the change in heat capacity obtained by extrapolation from the pre- and posttransition regions (Privalov & Khechinashvili, 1974).

Thermodynamic Analysis. The melting of C1s̄ in three different temperature ranges does not in itself mean that these three heat absorption peaks reflect the melting of three single cooperative units (domains). As has been shown (Privalov 1979, 1982), the cooperativity of a temperature-induced process can be analyzed only on the basis of a calorimetrically measured enthalphy function for each transition. In the simplest form, this can be done by comparison of the calorimetric enthalpy of a melting process (ΔH_m^{cal}), which is determined from the area of the heat absorption peak, with the van't Hoff enthalpy (ΔH_m^{vh}) determined by the sharpness of the melting process. The identity of these parameters for any given peak reflects the melting of a single cooperative unit (domain) that undergoes a transition between two macroscopic states. A ratio less than unity is usually connected with the sharpening of a peak due to aggregation, in which case one can only conclude the involvement of *at least* one domain. If the $\Delta H_m^{cal}/\Delta H_m^{vh}$ ratio is greater than unity, the transition definitely involves more than one domain, and their number can sometimes be deduced from the value of this ratio (Privalov, 1982).

The first step in such an analysis for C1s̄ is the the correct determination of the area and shape of the overlapping individual heat absorption peaks. This has been accomplished by an approach proposed earlier in which one or more irreversible transitions are eliminated from consideration by preincubating the sample at the appropriate temperature prior to scanning in the calorimeter (Medved et al., 1983). The results obtained are shown in Figure 7A. Curve a is the original scan for C1s̄ converted to a molar scale. Curve b is the scan of an identical sample that was preincubated for 1 h at 39 °C. This treatment largely eliminates the first peak from the profile, providing a clearer picture of the initial

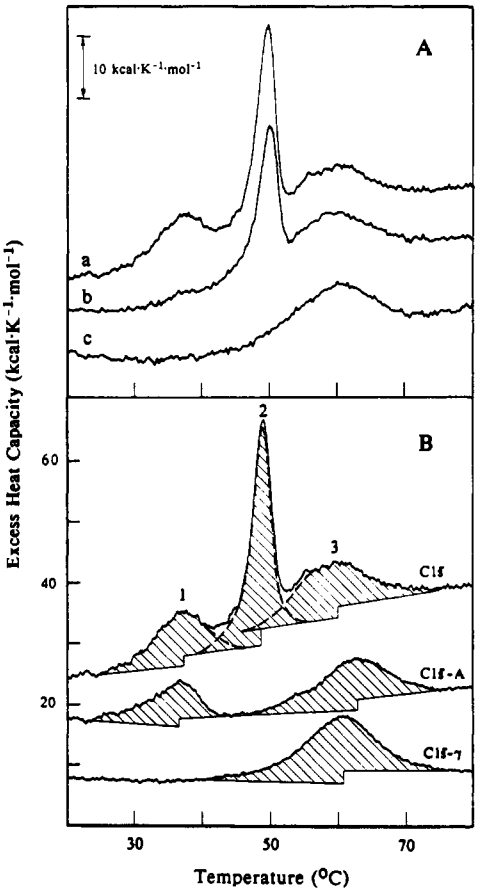

FIGURE 7: (A) Effect of preheating at various temperatures on the calorimetric curve for C1s̄. (Curve a) Original curve for C1s̄, as in Figure 3, but converted into molar units; (curve b) identical sample after preheating at 39 °C for 1 h; (curve c) identical sample preheated for 1 h at 48.5 °C. (B) Partial molar heat capacity of C1s̄, C1s̄-A fragment, and C1s̄-γ fragment. The shaded areas and broken lines indicate the manner in which the parameters summarized in Table I were manually obtained (see text).

portion of the second peak. Curve c was obtained with yet another sample that was preheated for 1 h at 48.5 °C such that only the third peak appears. Thus, curve a represents the melting of whole C1s̄, curve b the melting of the γB region, and curve c the melting of only the γ region. Comparison of these curves greatly facilitated the manual separation of the individual heat absorption peaks from the complex melting curve for whole C1s̄ and their subsequent thermodynamic analysis. The results are shown by the upper curve in Figure 7B, where the corresponding and less complicated analyses for C1s̄-A and C1s̄-γ are also shown.

Calorimetric and van't Hoff enthalpies obtained from these curves are given in the upper part of Table I. As seen, the

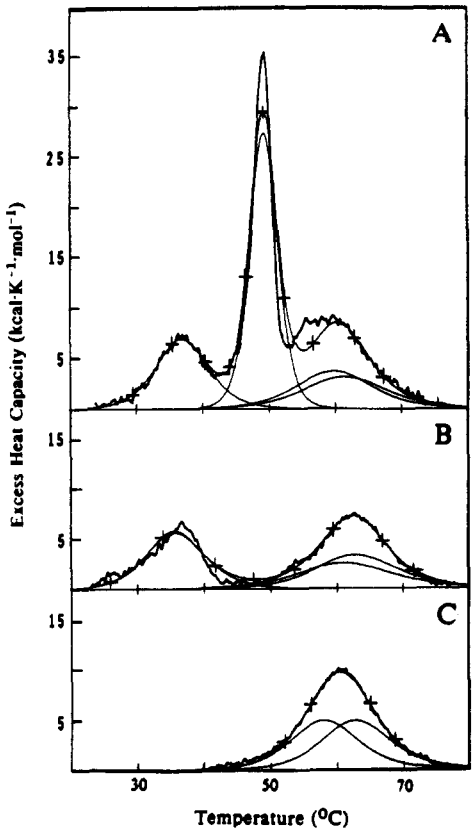

FIGURE 8: Deconvolution analysis of the excess heat capacity curves of C1s̄ (A), C1s̄-A (B), and C1s̄-γ (C) by the method of Freire and Biltonen (1978). Thick lines represent the experimental data. Thin lines with crosses represent the best fit to a series of sequential two-state transitions, each of which is shown by a thin line.

ratio $\Delta H_m^{cal}/\Delta H_m^{vh}$ for the first peak is close to unity, suggesting the melting of a single domain within the $\alpha\beta$ region. The second peak, which corresponds to the melting of the enzymatic B chain, yields a ratio of 0.7, again suggesting the melting of one domain. For the third peak, which corresponds to the melting of the γ region, this ratio is much greater than unity and has a value of 2.1 in the isolated C1s̄-γ fragment, where the transition is well-behaved and highly reversible. This indicates the presence of two independent domains with similar melting properties, presumably corresponding to the two similar motifs that comprise the γ region.

The calorimetrically measured enthalpy function was also analyzed directly by the recurrent procedures described in Freire and Biltonen (1978) and Privalov and Potekhin (1986). These procedures allow the observed melting curves to be deconvoluted directly to a number of either sequential (i.e., ordered) or independent (i.e., random) two-state transitions corresponding to the melting of individual domains in the protein. The results of the sequential analysis for C1s̄ and its fragments are illustrated in Figure 8 and in Table I (lower part). They are very similar to those obtained by the procedure described in the previous paragraphs. The denaturation process of C1s̄ can be described by four two-state transitions, one in the region of the first peak, another in the region of the second peak, and two in the region of the third peak. These latter two transitions were revealed also in the C1s̄-A and C1s̄-γ fragments. The second peak in C1s̄-A and the only peak of C1s̄-γ were both deconvoluted into two two-state transitions corresponding to the two transitions in the third peak of C1s̄. The first peak in C1s̄-A was described by a single two-state transition as in the corresponding peak in C1s̄. Thus, the analysis presented above indicates the existence of four independently folded domains in C1s̄ protein.

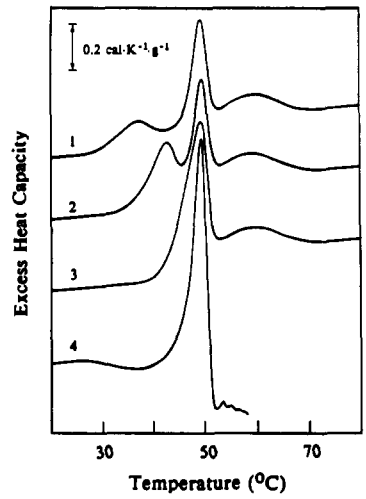

FIGURE 9: Effect of Ca^{2+} on the melting behavior of C1s̄. The curves represent C1s̄ in 0.05 M Tris-HCl, pH 7.2, and 0.22 M NaCl with 0.1 mM EDTA (1), without EDTA or Ca^{2+} (2), with 0.1 mM Ca^{2+} (3), or with 0.3 mM Ca^{2+} (4).

The endotherm for C1s̄-γ was also deconvoluted according to the independent (random) model. The results (not shown) were similar to those obtained by the sequential model, i.e., two transitions of essentially equal enthalpy separated by less than 1.5 °C. The two models were equivalent in their ability to fit the experimental curve. Thus, it was not possible to distinguish between ordered and random mechanisms of unfolding of the two SCR modules comprising this fragment.

Influence of Ca^{2+} on the Stability of the Individual Domains. It was previously shown that the first low-temperature transition arising from the interaction domain ($\alpha\beta$ region) is Ca^{2+} sensitive, while the second transition arising from the catalytic domain (B chain) is Ca^{2+} insensitive (Busby & Ingham, 1988). The effect of Ca^{2+} on the third transition, the transition of the γ region, is unknown. To clarify this relationship, we have studied the melting of C1s̄ in the presence of different concentrations of Ca^{2+}. Comparison of curves 1 and 2 in Figure 9 indicates that the mere absence of EDTA is sufficient to shift the low-temperature transition upward by several degrees, presumably due to residual divalent cations in the buffer. Addition of 0.1 mM $CaCl_2$ further shifts this transition into the region of transition 2. These effects are unique to the first transition; the positions of peaks 2 and 3 do not appear to be affected. In 0.3 M $CaCl_2$, the low-temperature transition is no longer visible and the apparent amplitude of peak 2 is significantly increased, indicating a further shift of peak 1 into this region. The profile is complicated by the exothermic effects of aggregation that cause a gradual decrease in the heat capacity function beginning near 28 °C and a sharp decrease above 50 °C. Further increases in the Ca^{2+} concentration caused dramatic aggregation that interfered with the recording of a melting curve. The results indicate that Ca^{2+} does not influence the stability of the two thermostable domains of the γ region or that of the catalytic or B chain domain. It therefore appears that the $\alpha\beta$ region is the only part of the C1s̄ molecule that binds Ca^{2+}.

Discussion

In this work we have utilized differential scanning calorimetry to characterize the denaturation process of C1s̄ and its fragments. The observed heat absorption peaks in C1s̄ are referred to as transitions 1, 2, and 3 in order of their increasing melting temperatures in the presence of EDTA. The first transition is assigned to the N-terminal region of the A chain.

The reasons for this assignment are (a) the transition occurs in C1s̄-A but not in C1s̄-γB, (b) it is strongly stabilized by Ca^{2+}, which is believed to bind in the α region (Arlaud et al., 1987; Villiers et al., 1985), and (c) a similar Ca^{2+} sensitive transition is seen by fluorescence methods in the isolated α fragment of C1r̄ (Busby & Ingham, 1987), whose amino acid sequence in 38% homologous to that of C1s̄ (Tosi et al., 1987). Transition 2 is assigned to the catalytic B chain since (a) it occurs in C1s̄-γB but not in C1s̄-A, from which most of the B chain is removed, and (b) it is associated with a loss of catalytic activity (Busby & Ingham, 1988). Transition 3 is assigned to the γ region of C1s̄ since (a) this is the only region common to C1s̄-A and C1s̄-γB where the transition is observed and (b) a similar transition was reproduced in C1s̄-γ, a fragment generated by enzymatic digestion of C1s̄-A under conditions where the less stable αβ region was entirely removed.

Transitions 1 and 2 were not reversible under the conditions employed in the heating experiments. However, the failure of the domains corresponding to transitions 1 and 2 to refold on cooling does not mean that these regions of the molecule are intrinsically metastable. It is more likely that secondary phenomena accompany the unfolding process and prevent or drastically retard the back reaction, as illustrated in

$$N \underset{k_{-1}}{\overset{k_1}{\rightleftharpoons}} D \xrightarrow{k_2} I$$

where N represents the native state, D represents the reversibly denatured state, and I represents the irreversibly denatured state. If k_1 and $k_{-1} \gg k_2$ and the sample is heated fast enough, or if the heat liberated or consumed by step 2 is relatively small, the results can be analyzed in terms of equilibrium thermodynamics, even though continued heating at or above the transition temperature may lead to completion of the postunfolding process and consequent failure to reproduce the given transition in a second scan (Privalov & Medved, 1982; Manly et al., 1985; Edge et al., 1985; Privalov & Potekhin, 1986; Sanches-Ruiz et al., 1988). In this connection, it can be pointed out that a 2-fold increase in the rate of heating of C1s̄ did not significantly affect the position or magnitude of the three peaks (not shown). This means that the enthalpy values reported in Table I can be regarded in the first approximation as correct ones. Nevertheless, for accurate interpretation one must keep in mind that if irreversible alteration of the unfolded state takes place, it can distort the shape of the melting curves, especially in the case of aggregation, which seems to be a common cause of irreversibility.

In the case of C1s̄ there was evidence that melting of the B chain was accompanied by an exothermic process, most likely aggregation, that caused a sharpening of peak 2 and an apparent deviation of the calculated values of ΔH_m^{cal} and ΔH_m^{vh} from the true values and to some underestimation of the $\Delta H_m^{cal}/\Delta H_m^{vh}$ ratio. The effects of this sharpening are most apparent in Figure 8A, where it was impossible to fit adequately the observed data in the region of the second peak with a theoretical two-state transition, and in the value of $\Delta H_m^{cal}/\Delta H_m^{vh} = 0.7$ obtained for this peak (Table I). The problem was much worse in the case of the isolated γB fragment, where aggregation was so severe as to preclude any thermodynamic analysis at all, especially at pH 7.2 (dotted curve, Figure 3, bottom). This tendency of the isolated fragment to aggregate more than the parent protein may be related to the substantial decrease in net charge that would be expected from the removal of domains I, II, and III (Tosi et al., 1987). Meanwhile, it can be pointed out that the B chain of C1s̄ is homologous to trypsin and chymotrypsin, which are single-domain proteins of similar size that melt with an enthalpy (Privalov, 1982) close to that reported in Table I for transition 2 in C1s̄. This supports our conclusion that the B chain of C1s̄ forms an independently folded domain that melts in the second transition.

With transition 1, aggregation was less of a problem, at least with whole C1s̄, as documented previously by light scattering and by exclusion chromatography of samples that had been held for 30 min at temperatures at or near the midpoint (Busby & Ingham, 1988). A small amount of aggregation or other exothermic process seems to occur with C1s̄-A, as evidenced by the observed assymetry of the first transition (Figure 3) and by the $\Delta H_m^{cal}/\Delta H_m^{vh}$ ratio of 0.7 (Table I). The assymetry becomes obvious on comparison of the experimental curve with the theoretical one for a two-state transition (Figure 8B). Thus, one cannot exclude the possibility of more than one domain melting in this region. The amino acid sequence shows three motifs in the N-terminal region, suggesting up to three domains (Figure 1). One of these, motif II, is homologous to epidermal growth factor (EGF) (Mackinnon et al., 1987; Tosi et al., 1987). EGF itself forms an extremely stable domain, requiring high concentrations of guanadinium chloride to effect its melting (Holladay et al., 1976). It is thus possible that motif II does not unfold under the conditions reached in our experiments. This would imply that the low-temperature transition in C1s̄ and C1s̄-A involves motifs I and/or III, which are homologous to each other and unique to C1s̄ and C1r̄. We have not yet succeeded in isolating smaller fragments from this region in quantities sufficient to define the origin of this transition. However, the appearance of two discrete intermediate fragments, fr.1 and fr.2, (Figure 4), during the early stage of digestion of C1s̄-A by plasmin or chymotrypsin indicates the presence of protease-sensitive regions separating less vulnerable ones, consistent with published observations on whole C1s̄ (Villiers et al., 1985). The occurrence of discrete fragments during digestion with multiple proteases is good evidence for a complex domain structure.

Peak 3 had a $\Delta H_m^{cal}/\Delta H_m^{vh}$ ratio close to 2.0 in C1s̄ and its fragments and was readily resolved into two closely spaced two-state transitions, indicating that each of the SCR units comprising the γ region is independently folded (Table I, Figure 8). Had they not been independently folded, one would expect a ratio of less than two, reflecting the cooperativity between them. The highly reversible nature of transition 3 allowed us to determine the thermodynamic properties of the γ region with greater accuracy and in greater detail than for the irreversible melting of αβ and B chain regions of C1s̄. The magnitude of the experimentally observed change in heat capacity between the native and denatured states of C1s̄-γ ($\Delta_m C_p = 0.104$ cal·K^{-1}·g^{-1}, Figure 6) suggests that unfolding of the two SCR units is accompanied by the exposure of a large number of nonpolar residues (Privalov, 1979, 1982). In fact, extrapolation of the specific enthalpy Δh_m, for this fragment to 110 °C by

$$\Delta h_m(T) = \Delta h_m(T_m) + \int_T^{T_m} \Delta_m C_p \, dT$$

gives us a value of Δh_m (110 °C) = 10.9 cal·g^{-1}, which is close to the value of 13 cal·g^{-1} observed for the family of typical globular proteins (Privalov & Khechinashvili, 1974; Privalov, 1979). The agreement is even better if we take into account that a portion of the mass of C1s̄-γ is contributed by carbohydrate together with a residual piece of the B chain that is most likely unstructured and does not take part in the melting process. Thus, it can be concluded that the two domains formed by the γ region of C1s̄ are of the globular type; i.e.,

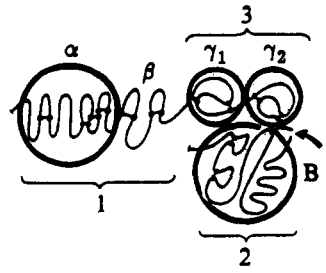

FIGURE 10: Schematic illustration of the independently folded domains of C1s. The α, β, and B regions are labeled according to the scheme in Figure 1. γ_1 and γ_2 correspond to the two homologous repeat units within the γ region. The numbers 1, 2, and 3 denote the regions that melt in the first, second, and third peaks, respectively. The arrow indicates the site of the cleavage that generates enzyme from proenzyme, producing the A and B chains.

they are compact and have a well-developed hydrophobic core.

To summarize, on the basis of the calorimetric data and the results of proteolysis, we conclude that the C1s protein consists of at least four independently folded domains as illustrated schematically in Figure 10. The domain(s) melting in the first peak is (are) located within the αβ region of the A chain; another domain, which melts in the second peak, is formed by the B chain. The γ region of C1s, consisting of the two homologous repeat structures (SCRs), forms two thermostable domains that melt independently in the third peak. As was mentioned in the introduction, SCR structures have been found in several proteins (Reid et al., 1986; Klickstein et al., 1987). Whether they also form independent domains in these other proteins remains to be determined. Since the isolated domains do not reveal dramatic changes in stability as compared to their melting behavior in the parent C1s molecule, noncovalent interactions between domains must be weak in comparison to the intradomainal interactions. This does not preclude intramolecular associations between domains that may be sufficiently strong to account for the smaller number of globular domains seen in the electron microscope (Villiers et al., 1985). The findings presented here may stimulate new efforts to visualize additional structurally distinct lobes under appropriate conditions.

ACKNOWLEDGMENTS

We thank Dr. Dudley Strickland for critical advice during the course of this work. We also thank Mary Migliorini, Debra Milasincic, and Oleg Yatsuk for technical assistance.

Registry No. C1s, 80295-70-1.

REFERENCES

Arlaud, G. J., Colomb, M. G., & Gagnon, J. (1987) *Immunol. Today 8*, 106–111.

Bing, D. H., Andrews, J. M., Morris, K. M., Cole, E., & Frish, V. (1980) *Prep. Biochem. 10*, 269–296.

Busby, T. F., & Ingham, K. C. (1987) *Biochemistry 26*, 5564–5571.

Busby, T. F., & Ingham, K. C. (1988) *Biochemistry 27*, 6127–6135.

Cooper, N. R. (1985) *Adv. Immunol. 37*, 151–216.

Edelhoch, H. (1967) *Biochemistry 6*, 1948–1954.

Edge, V., Allewell, N. M., & Sturtevant, J. M. (1985) *Biochemistry 24*, 5899–5906.

Freire, E., & Biltonen, R. L. (1978) *Biopolymers 17*, 463–479.

Holladay, L. A., Savage, C. R., Jr., Cohen, S. & Puett, D. (1976) *Biochemistry 15*, 2624–2633.

Klickstein, L. B., Wong, W. W., Smith, J. A., Weis, J. H., & Fearon, D. T. (1987) *J. Exp. Med. 165*, 1095–1112.

Kolb, W. P., Kolb, L. M., & Podack, E. R. (1979) *J. Immunol. 122*, 2103–2111.

Lennick, M., Brew, S. A., & Ingham, K. C. (1985) *Biochemistry 24*, 2561–2568.

Mackinnon, C. M., Carter, P. E., Smyth, S. J., Dunbar, B., & Fothergill, J. E. (1987) *Eur. J. Biochem. 169*, 547–553.

Manly, S. P., Matthews, K. S., & Sturtevant, J. M. (1985) *Biochemistry 24*, 3842–3846.

Medved, L. V., Privalov, P. L., & Ugarova, T. P. (1982) *FEBS Lett. 146*, 339–342.

Medved, L. V., Gorkun, O. V., & Privalov, P. L. (1983) *FEBS Lett. 160*, 291–295.

Privalov, P. L. (1979) *Adv. Protein Chem. 33*, 167–241.

Privalov, P. L. (1982) *Adv. Protein Chem. 35*, 1–104.

Privalov, P. L., & Khechinashvili, N. N. (1974) *J. Mol. Biol. 86*, 665–684.

Privalov, P. L., & Medved, L. V. (1982) *J. Mol. Biol. 159*, 665–683.

Privalov, P. L., & Potekhin, S. A. (1986) *Methods Enzymol. 131*, 4–51.

Reid, K. B. M., Bentley, D. R., Campbell, R. D., Chung, L. P., Sim, R. B., Kristensen, T., & Tack, B. F. (1986) *Immunol. Today 7*, 230–234.

Sanchez-Ruiz, J. M., Lopez-Lacomba, J. L., Cortijo, M., & Mateo, P. O. (1988) *Biochemistry 27*, 1648–1652.

Schumaker, V. N., Zavodszky, P., & Poon, P. H. (1987) *Am. Rev. Immunol 5*, 21–24.

Sim, R. B., Porter, R. R., Reid, K. B. M., & Gigli, I. (1977) *Biochem. J. 163*, 433–449.

Stenflo, J., Lundwall, A., & Dahlback, B. (1987) *Proc. Natl. Acad. Sci. U.S.A. 84*, 368–372.

Tosi, M., Duponchel, C., Meo, T., & Julier, C. (1987) *Biochemistry 26*, 8516–8524.

Villiers, C. L., Arlaud, G. J., & Colomb, M. G. (1985) *Proc. Natl. Acad. Sci. U.S.A. 82*, 4477–4481.